Sensitivity of Latent Heat Flux from PILPS Land-Surface Schemes to Perturbations of Surface Air Temperature

Weiqing Qu,[a] A. Henderson-Sellers,[a] A. J. Pitman,[b] T. H. Chen,[c] F. Abramopoulos,[d] A. Boone,[e]
S. Chang,[f] F. Chen,[g] Y. Dai,[h] R. E. Dickinson,[i] L. Dümenil,[j] M. Ek,[k] N. Gedney,[l] Y. M. Gusev,[m] J. Kim,[n]
R. Koster,[o] E. A. Kowalczyk,[p] J. Lean,[q] D. Lettenmaier,[r] X. Liang,[s] J.-F. Mahfouf,[t]
H.-T. Mengelkamp,[u] K. Mitchell,[g] O. N. Nasonova,[m] J. Noilhan,[v] A. Robock,[w] C. Rosenzweig,[d]
J. Schaake,[x] C. A. Schlosser,[w] J.-P. Schulz,[j] A. B. Shmakin,[y] D. L. Verseghy,[z] P. Wetzel,[e] E. F. Wood,[s]
Z.-L. Yang,[i] and Q. Zeng[h]

ABSTRACT

In the PILPS Phase 2a experiment, 23 land-surface schemes were compared in an off-line control experiment using observed meteorological data from Cabauw, the Netherlands. Two simple sensitivity experiments were also undertaken in which the observed surface air temperature was artificially increased or decreased by 2 K while all other factors remained as observed. On the annual timescale, all schemes show similar responses to these perturbations in latent, sensible heat flux, and other key variables. For the 2-K increase in temperature, surface temperatures and latent heat fluxes all increase while net radiation, sensible heat fluxes, and soil moistures all decrease. The results are reversed for a 2-K temperature decrease. The changes in sensible heat fluxes and, especially, the changes in the latent heat fluxes are not linearly related to the change of temperature. Theoretically, the nonlinear relationship between air temperature and the latent heat flux is evident and due to the convex relationship between air temperature and saturation vapor pressure. A simple test shows that, the effect of the change of air temperature on the atmospheric stratification aside, this nonlinear relationship is shown in the form that the increase of the latent heat flux for a 2-K temperature increase is larger than its decrease for a 2-K temperature decrease. However, the results from the Cabauw sensitivity experiments show that the increase of the latent heat flux in the +2-K experiment is smaller than the decrease of the latent heat flux in the −2-K experiment (we refer to this as the asymmetry). The analysis in this paper shows that this inconsistency between the theoretical relationship and the Cabauw sensitivity experiments results (or the asymmetry) is due to (i) the involvement of the β_g formulation, which is a function of a series stress factors that limited the evaporation and whose values change in the ±2-K experiments, leading to strong modifications of the latent heat flux; (ii) the change of the drag coefficient induced by the changes in stratification due to the imposed air temperature changes (±2 K) in parameterizations of latent heat flux common in current land-surface schemes. Among all stress factors involved in the β_g formulation, the soil moisture stress in the +2-K experiment induced by the increased evaporation is the main factor that contributes to the asymmetry.

[a] Royal Melbourne Institute of Technology, Melbourne, Australia
[b] School of Earth Sciences, Macquarie University, Sydney, Australia
[c] Australian Oceanographic Data Centre, Sydney, Australia
[d] Science Systems and Applications Inc., New York, New York
[e] Mesoscale Dynamics and Precipitation Branch, NASA/Goddard Space Flight Center, Greenbelt, Maryland
[f] Phillips Laboratory (PL/GPAB), Hanscom AFB, Massachusetts
[g] Development Division, National Centers for Environmental Prediction/NOAA, Camp Springs, Maryland
[h] Institute of Atmospheric Physics, Academy of Science, Beijing, People's Republic of China
[i] Institute of Atmospheric Physics, The University of Arizona, Tucson, Arizona
[j] Max-Planck-Institut für Meteorologie, Hamburg, Germany
[k] Royal Netherlands Meteorological Institute, De Bilt, the Netherlands
[l] Meteorology Department, Reading University, Reading, United Kingdom

[m] Institute of Water Problems, Moscow, Russia
[n] Lawrence Livermore National Laboratory, Livermore, California
[o] Hydrological Sciences Branch, NASA/GSFC, Greenbelt, Maryland
[p] Division of Atmospheric Research, CSIRO, Aspendale, Victoria, Australia
[q] Hadley Centre for Climate Prediction and Research, Meteorological Office, Berkshire, United Kingdom
[r] Department of Civil Engineering, University of Washington, Seattle, Washington
[s] Department of Civil Engineering and Operations Research, Princeton University, Princeton, New Jersey
[t] ECMWF, Reading, United Kingdom
[u] Department of Physics, GKSS—Research Center, Geesthacht, Germany
[v] Météo-France/CNRM, Toulouse, France
[w] Department of Meteorology, University of Maryland, College Park, Maryland
[x] Office of Hydrology, NWS/NOAA, Silver Spring, Maryland
[y] Institute of Geography, Moscow, Russia
[z] Climate Research Branch, Atmospheric Environment Service, Downsview, Ontario, Canada

Corresponding author address: Dr. Weiqing Qu, Department of Mathematics, Royal Melbourne Institute of Technology, GPO Box 2476V, Melbourne, Victoria 3001, Australia.
E-mail: rmawq@gauss.ma.rmit.edu.au

1. Introduction

In order to improve the understanding of the parameterization of land surface processes, the Project for Intercomparison of Land-Surface Parameterization Schemes (PILPS) was initiated in 1992 as a World Climate Research Programme project. The overall goals of PILPS are to improve the performance of land-surface schemes, as they are used in climate and weather prediction models. The progress to date and planned future activities of PILPS are described in detail by Henderson-Sellers et al. (1995).

In Phase 2 of PILPS, land-surface schemes are being compared in off-line experiments that employ observed data. The Cabauw experiment (Phase 2a) used observation from Cabauw, the Netherlands (51°58′N, 4°56′E) (Beljaars and Viterbo 1994; Beljaars and Bosveld 1997), as the atmospheric forcing to drive 23 land-surface schemes (Table 1). Point-based observations of surface energy fluxes, net radiation, and upward longwave radiation data were used for validation of the simulations (Chen et al. 1997). In addition to these intercomparisons, two sensitivity experiments were undertaken using modified versions of the Cabauw forcing in which the surface air temperature was increased or decreased by 2 K at every model time step. Hereafter, the experiment with +2-K forcing is referred to as "Plus2" and that with −2-K forcing as "Minus2."

The results from the off-line simulations in previous phases of PILPS (Pitman et al. 1993; Shao and Henderson-Sellers 1996) show that there were large discrepancies among the existing land-surface schemes in terms of the partitioning of surface net radiation into sensible heat and latent heat flux and partitioning of precipitation into evapotranspiration and soil water components (soil water storage, runoff, and drainage). Any attempt to understand the reasons for these discrepancies requires a systematic examination and intercomparison of individual parameterizations and processes within the models. To address the similar diversity in GCM simulations (i.e., when GCM simulations showed quite differing climatic responses to prescribed forcing such as increasing CO_2 (Schlesinger and Mitchell 1987), Wetherald and Manabe (1988) and Hansen et al. (1981) used a procedure in which basic variables, such as temperature, water vapor, surface albedo, and cloud cover, were individually varied to assess individual feedback processes. Cess and Potter (1988) presented a computationally more efficient means for both understanding and intercomparing climate feedback mechanisms in GCM simulations by using surface temperature perturbations as a surrogate climatic change for the purpose of studying atmospheric feedback processes.

Such techniques are also very useful for understanding and intercomparing the land-surface parameterization schemes. The sensitivity experiments discussed in this paper are analogous to the Cess et al. (1990) experiments, which evaluated cloud forcing sensitivities in GCMs by artificially increasing and then decreasing prescribed sea surface temperatures by 2 K. The purpose of these sensitivity experiments was to obtain a first-order estimate of the sensitivity of PILPS schemes to changed air temperatures and to determine whether different schemes respond to such changes differently and the extent to which any differences could be traced to different parameterizations. Although different experiments in which other forcing variables are also altered can be constructed, this paper describes only these first-order tests.

In this paper, the sensitivity of latent heat fluxes in current land-surface schemes to the change of air temperature will be described and analyzed. The behavior of the latent and sensible heat flux is discussed in section 2a, including the theoretical aspects of the relationship between latent heat flux and air temperature. The effect of the "classic β" formulation on the parameterization of latent heat is discussed in section 3a, together with the influence of stress factors in the sensitivity experiments in section 3b. Finally, some conclusions are drawn in section 4.

2. Sensitivity of latent heat fluxes in the Plus2 and the Minus2 experiments

a. Behavior of the latent and sensible heat flux

Since the incoming radiation was not altered in the sensitivity experiments discussed here, the increase in air temperature must lead to changes in the latent or sensible heat. This is achieved by an adjustment of surface temperature. Figure 1 shows the differences in the annual mean effective temperatures, T_s (the combined mean surface radiative temperature of the canopy and the ground) between Plus2 and Control (i.e., $T_s^{+2} - T_s^C$), and that between Minus2 and Control (i.e., $T_s^{-2} - T_s^C$) for all 23 PILPS schemes. It can be seen that annual mean effective surface temperature increases or decreases by about 1 K when air temperature increases or decreases by 2 K. BUCKET shows the largest annual mean increase (1.68 K) and the U.K. Meteorological Office (UKMO) the smallest (0.73 K) in Plus2 while SPONSOR showing the largest annual mean decrease (1.55 K) and the Goddard Institute of Space Sciences (GISS), ISBA the smallest (0.83 K) in Minus2. It should be noted that the change of the surface temperature with the increase or decrease of air temperature is the key mechanism that causes the change in the other quantities analyzed here (Qu et al. 1996).

Generally, most of the schemes exhibit similar, but opposite, behavior in Plus2 and Minus2. Figure 2 shows the difference of latent heat flux L and sensible heat flux H (W m^{-2}) between Plus2 (Minus2) and Control for all 23 land-surface schemes. Compared to the control experiment, latent heat flux increases by about 6 W m^{-2} in Plus2, with BUCKET showing the lowest increase

TABLE 1. List of models participating in PILPS phase 2a and some basic information about these landsurface schemes.

Model	Contact	Number of layers for — C^a	T^b	S^c	R^d	Time step	Spinup time	Major purpose	C^a	Philosophy for — T^b	S^c	Reference
BASE	C. E. Desborough, A. J. Pitman	1	3	3	3	20 min	13 yr	GCM	aerodynamic	heat diffusion	Philip–de Vries	Cogley et al. (1990)[e]
BATS	R. E. Dickinson, Z.-L. Yang	1	2	3	2	30 min	3 yr	GCM	aerodynamic	force–restore	Darcy's law	Dickinson et al. (1986, 1993)
BUCKET	C. A. Schlosser, A. Robock	0	1	1	1	30 min	1 yr	GCM	implicit	heat balance	bucket + variation	Robock et al. (1995)
CAPS	S. Chang, M. Ek	1	3	3	2	30 min	1 yr	GCM	Penman–Monteith	heat diffusion	Darcy's law	Mahrt and Pan (1984), Pan and Mahrt (1987)
CAPSLLNL	J. Kim	1	2	3	1	5 min	10 yr	GCM–mesoscale	full energy balance	heat diffusion	Darcy's law + diffusion	Mahrt and Pan (1984), Kim and Ek (1995)
CAPSNMC	K. Mitchell, F. Chen	1	3	3	2	30 min	3 yr	GCM–mesoscale	Penman–Monteith	heat diffusion	Darcy's law	Mahrt and Pan (1984), Pan and Mahrt (1987), Chen et al. (1996)
CLASS	D. Verseghy	1	3	3	3	30 min		GCM	aerodynamic	heat diffusion	Darcy's law	Verseghy (1991), Verseghy et al. (1993)
CSIRO9	E. Kowalczyk, J. R. Garratt	1	3	2	1	30 min		GCM	aerodynamic	heat diffusion	force–restore	Kowalczyk et al. (1991)
ECHAM	L. Dümenil, J.-P. Schulz	1	5	1	1	30 min	5 yr	GCM	aerodynamic	heat diffusion	bucket + variation	Dümenil and Todini (1992)
GISS	F. Abramopoulos	1	6	6	6	30 min	13 yr	GCM	aerodynamic	aerodynamic	Darcy's law	Abramopoulos et al. (1988)
IAP94	Q. Zeng, Y. Dai	1	3	3	2	1 h	60 yr	GCM	Penman–Monteith	heat diffusion	Darcy's law	Dai and Zeng (1996)
ISBA	J. Noilhan, J.-F. Mahfouf	1	2	2	1	5 min		GCM–mesoscale	aerodynamic	force–restore	force–restore	Noilhan and Planton (1989)
MOSAIC	R. Koster	1	2	3	2	5 min	6 yr	GCM	aerodynamic	force–restore	Darcy's law	Koster and Suarez (1992)
PLACE	P. Wetzel, A. Boone	1	7	5	2	30 min		flexible	Ohm's law analogy	heat diffusion	Darcy's law	Wetzel and Boone (1995)
SECHIBA2	J. Polcher, K. Laval	1	7	2	1	30 min	2 yr	GCM	aerodynamic	heat diffusion	Choisnel	Ducoudre et al. (1993)
SEWAB	H.-T. Mengelkamp	1	6	6	1	10–30 s	3 yr	mesoscale	aerodynamic	heat diffusion	diffusion of water content	Mengelkamp et al. (1997)
SPONSOR	A. B. Shmakin	1	1	2	2	24 h	3 yr	GCM	aerodynamic	energy balance	variation	Shmakin et al. (1993)
SSiB	Y. Xue, C. A. Schlosser	1	2	3	1	30 min	2 yr	GCM–mesoscale	aerodynamic	force–restore	diffusion	Xue et al. (1991)
SWAP	Y. M. Gusev, O. N. Nasonova	1	2	1	1	24 h	2 yr	mesoscale	energy + water balance + aerodynamic	water balance	water balance	Gusev and Nasonova (1996)
SWB	J. Schaake, V. Koren	0	3	2	2	30 min	3 yr	mesoscale	Penman–Monteith	heat diffusion	bucket + variation	Schaake et al. (1996)
UGAMP2	N. Gedney	1	3	3	2	30 min		GCM	aerodynamic	heat diffusion	Darcy's law	Gedney (1995)
UKMO	J. Lean	1	4	4	4	30 min	1 yr	GCM	Penman–Monteith	heat diffusion	Darcy's law	Warrilow et al. (1986)
VIC-3L	X. Liang, E. Wood, D. Lettenmaier	1	2	3	3	1 h	2 yr	GCM–mesoscale	Penman–Monteith	heat diffusion	variable infiltration capacity + more	Gregory and Smith (1994), Liang et al. (1994; 1996)

[a] Canopy; [b] soil temperature; [c] soil moisture; [d] roots; [e] the basic philosophy of BASE is described in the reference and a full description of the scheme is in preparation.
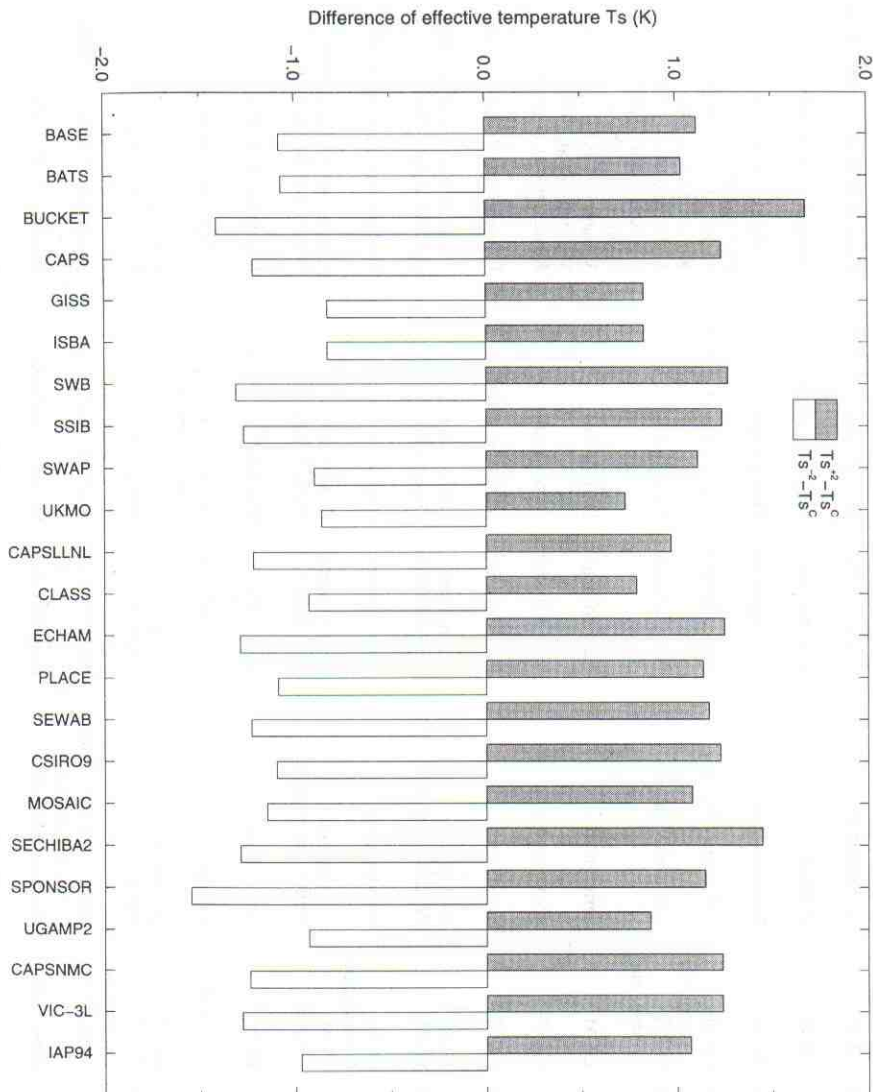
FIG. 1. Difference of annual mean surface temperature between Plus2 and control, as well as that between Minus2 and control for 23 land-surface schemes.

(2.1 W m^{-2}) and CAPS the highest (9.6 W m^{-2}), and decreases by about 11 W m^{-2} in Minus2, with UGAMP2 showing the lowest decrease (5.6 W m^{-2}) and VIC-3L the highest (17.0 W m^{-2}) (Fig. 2a). SPONSOR is the only scheme that produces a small decrease of latent heat flux in Plus2. A possible reason for this behavior will be discussed in section 3b(3). Sensible heat flux decreases by about 12 W m^{-2} in Plus2, with CAPS showing the largest decrease (16.2 W m^{-2}) and SPONSOR the lowest (4.7 W m^{-2}), and increases about 16 W m^{-2} in Minus2, with VIC-3L showing the highest increase (23.7 W m^{-2}) and SWAP the lowest (9.9 W m^{-2}) (Fig. 2b). It should be noted here that for Plus2 the annual means of sensible and latent heat fluxes have ranges across the schemes of 31 and 23 W m^{-2}, respectively, and for Minus2 of 24 and 28 W m^{-2}, respectively. These ranges are of a similar magnitude as

those for the control experiment, which is significantly larger than the uncertainties of the measurements (Chen et al. 1997). After Beljaars and Bosveld (1997), the observational errors of the Cabauw dataset are within ±5 W m^{-2} for sensible heat flux and ±10 W m^{-2} for surface net radiation and latent heat flux.

The changes in the latent heat fluxes follow from the dependence of the latent heat flux on the specific humidity gradient. In many PILPS schemes, the latent heat flux is parameterized as

$$L = \beta_g \times L_s, \qquad (1)$$

where L_s is the potential evaporation (scaling evaporation) and β_g is a function of a series of stress factors that limit the evaporation. For most of the schemes in PILPS, L_s and sensible heat fluxes (H) are parameterized as follows:
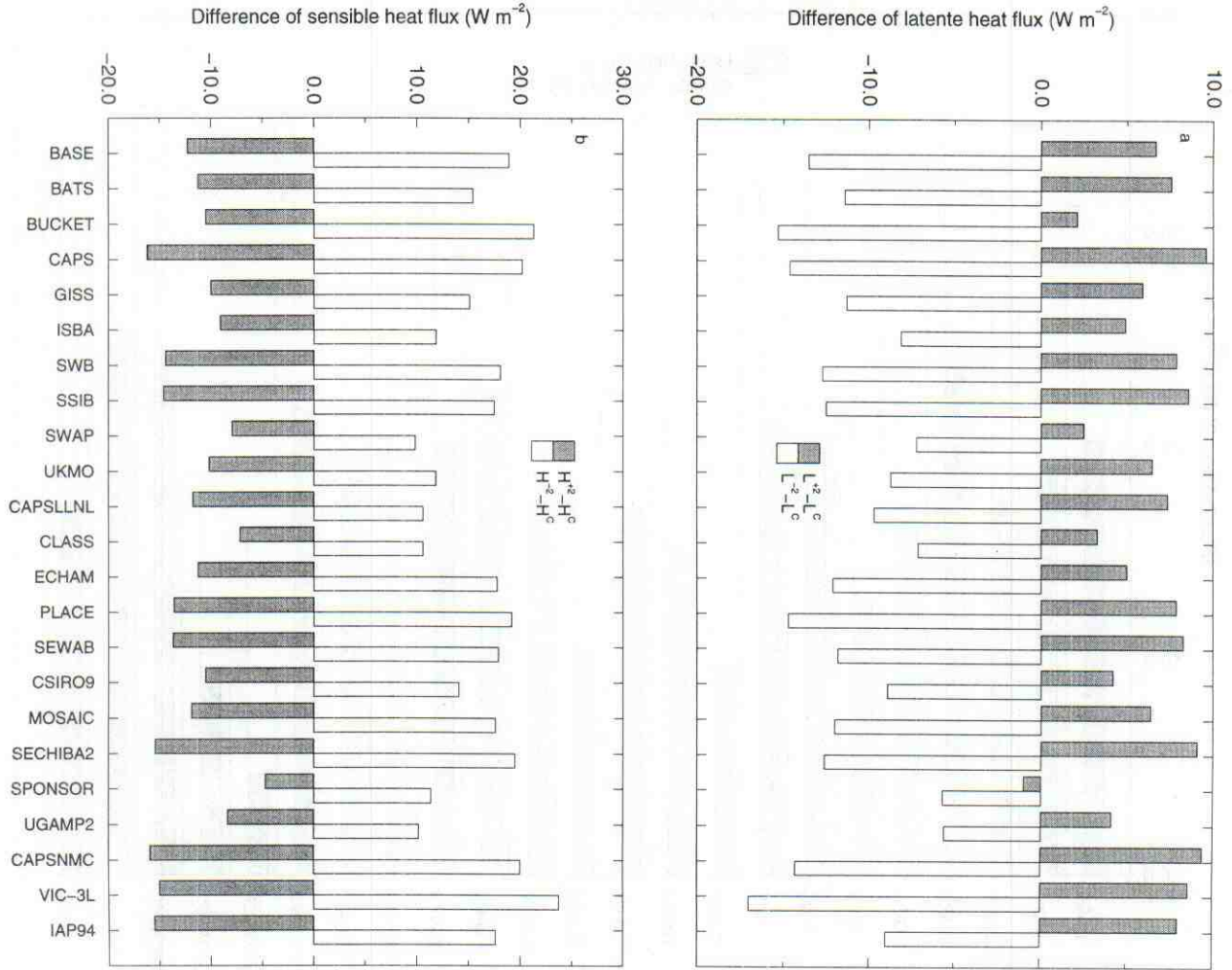
Difference of sensible heat flux (W m^{-2})   Difference of latente heat flux (W m^{-2})

FIG. 2. Difference of annual mean (a) latent heat flux L and (b) sensible heat flux H (W m^{-2}) between Plus2 (Minus2) and control for 23 land-surface schemes.

$$L_s = \lambda \rho U C_E [q_*(T_s) - q_a] \qquad (2)$$

and

$$H = \rho U C_H c_p (T_s - T_a), \qquad (3)$$

where λ is the latent heat of vaporization, q_* is saturation specific humidity, q_a is the specific humidity of air at reference height, T_s is the surface temperature (ground and/or canopy temperature), T_a is the air temperature at reference height, ρ is air density, U is the wind speed at reference height, and C_E and C_H are drag coefficients for latent and sensible heat fluxes, respectively. Ignoring the effects of β_g and the drag coefficient, the increases of T_s in Plus2, for example, leads to an increase of latent heat flux [because q_a and U in Eq. (2) are unchanged in the sensitivity experiments and the change in ρ is negligibly small]. For sensible heat flux [Eq. (3)], both T_s and T_a are increased for Plus2. However, since the increase of T_s induced by the increase of T_a is always smaller than the increase of T_a itself, the net effect is that sensible heat flux decreases in Plus2.

On the other hand, if air temperature is decreased by 2 K, T_s will decrease. Thus latent heat flux decreases and sensible heat flux increases.

Figure 3 shows the differences of L and H between Plus2 and Minus2. It can be seen that $|H^{+2} - H^{-2}|$ is larger than $|L^{+2} - L^{-2}|$ for all schemes; that is, sensible heat flux is more sensitive to the prescribed change of air temperature than latent heat flux. This is because of the linear relationship between H and T_s, which changes with the change of air temperature [Eq. (3)]. It can also be seen that if L of a certain scheme is sensitive to the change of air temperature, H is also sensitive.

The interesting result with regard to the behavior of latent heat flux is that the increases or decreases of latent heat flux in Plus2 and Minus2 are not linear with respect to the prescribed equal and opposite changes in air temperature ($+2$ K and -2 K). Figure 4 illustrates this nonlinearity. For clarity, 6 out of 23 schemes are shown, representative of median (UKMO, CLASS, SSIB, CSIRO9, ECHAM) and extreme (BUCKET) performance in the
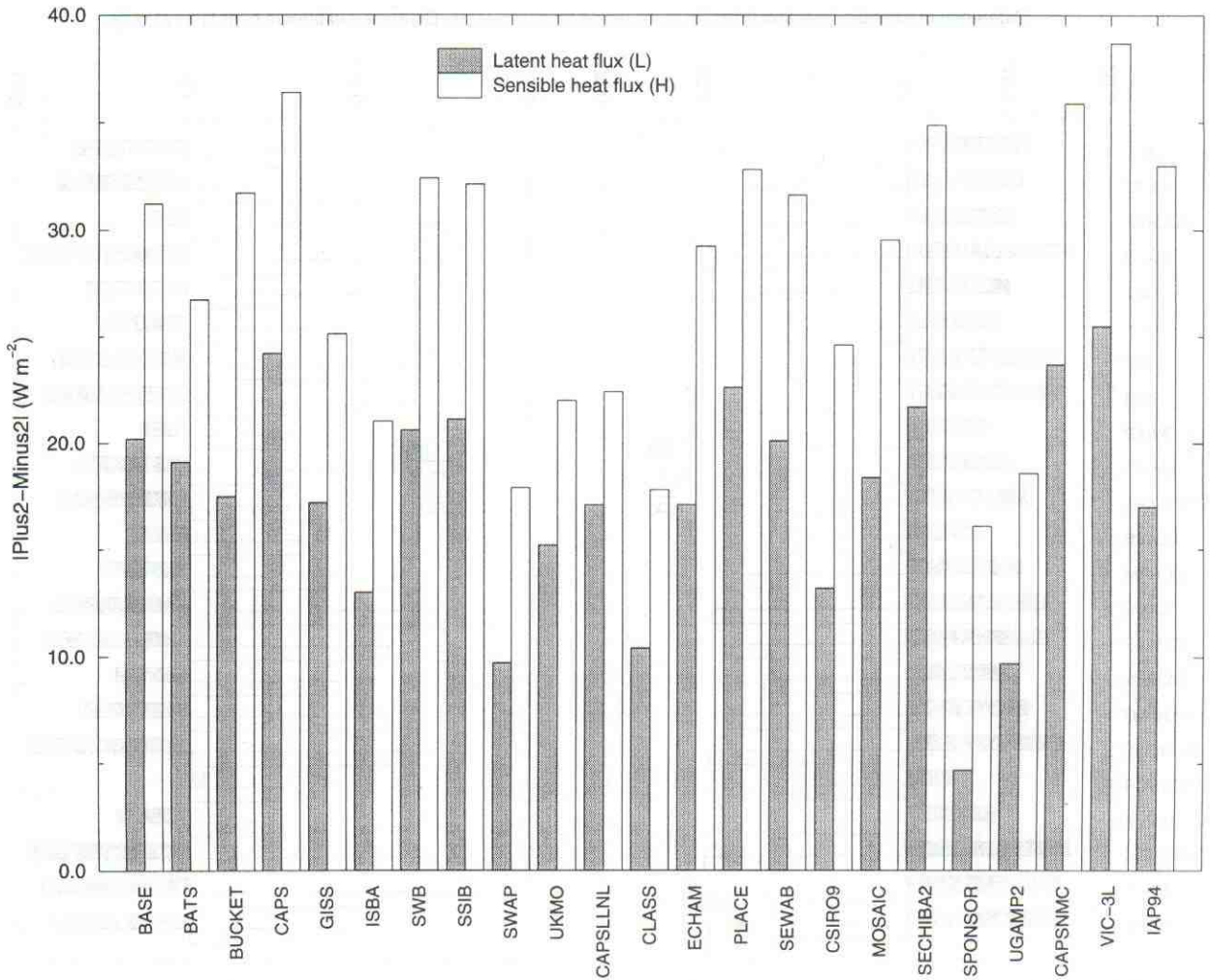
FIG. 3. Difference between annual mean latent heat flux and sensible heat flux (W m^{-2}) in Plus2 and those in Minus2 for 23 land-surface schemes.

control experiment (cf. Chen et al. 1997). For latent heat flux, the nonlinear relation to the change of air temperature is evident.

The crucial point here is that for most schemes the nonlinear relationship between latent heat flux and air temperature is shown by the increase of latent heat flux in Plus2 being much smaller than the decrease of latent heat flux in Minus2 (Fig. 2a). If we define

$$r_L = \frac{|L^{+2} - L^C|}{|L^{-2} - L^C|}, \qquad (4)$$

this result can also be described as

$$r_L < 1. \qquad (5)$$

In the following sections, the theoretical aspects of the relationship between L_s and air temperature will be illustrated through an investigation of the formulation of L_s [Eq. (2)], and then we try to explain the behavior of latent heat flux in the Plus2 and Minus2 Cabauw experiments.

b. Theoretical aspects of the relationship between L_s and air temperature

Equation (2) shows clearly that there is a nonlinear relation between surface temperature and L_s induced by the nonlinearity between surface temperature and saturation specific humidity. A numerical evaluation of Eq. (2) will be used here to illustrate the response of L_s to the change of air temperature. Fixing all variables in Eq. (2) except T_s and λ (λ changes with T_s) and assuming $\rho = 1.292$ (kg m^{-3}), $U = 5.0$ (m s^{-1}), $C_E = 0.00597$ (appendix of Chen et al. 1997), $q_a = 0.005$ (kg kg^{-1}), we allow T_s to increase or decrease 1 K because Fig. 1 shows that annual mean effective surface temperature increases or decreases by about 1 K when air temperature increases or decreases by 2 K. These changes in T_s are imposed upon a base surface temperature that varies from $-10°$ to 30°C to match the annual range of air temperature in Cabauw (Beljaars and Bosveld 1997). In this numerical test, we use the symbol L_s^{+1} to represent
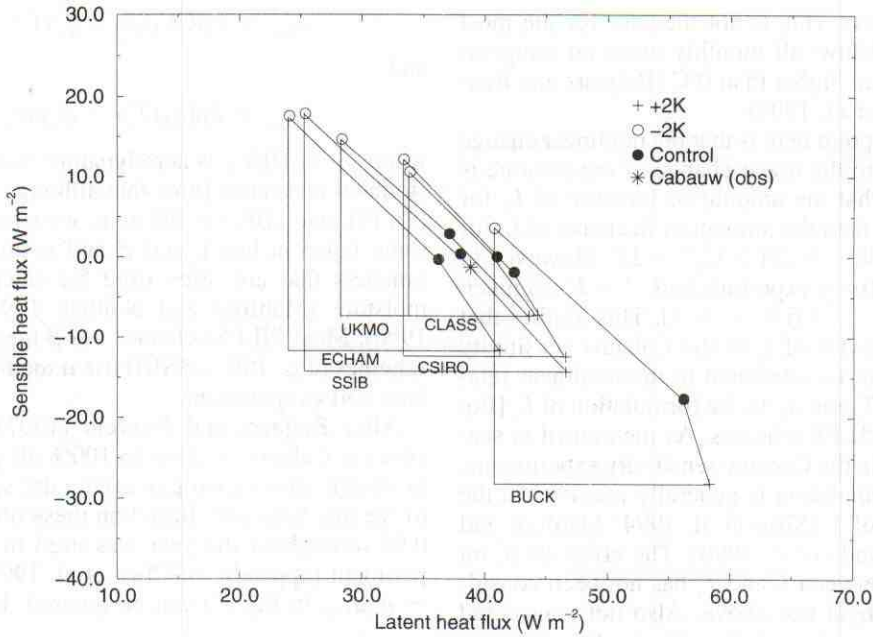
FIG. 4. Annual sensible heat flux vs latent heat flux for Cabauw control experiment, Plus2, and Minus2 for six chosen schemes that are representative of medium (UKMO, CLASS, SSIB, CSIRO9, ECHAM) and extreme (BUCKET) performance in the control experiment.

L_s for T_s increased by 1 K, L_s^{-1} to represent L_s for T_s decreased by 1 K, and L_s^c for control.

Figure 5 shows the difference (absolute values) between L_s^{+1} and L_s^C and the difference between L_s^{-1} and L_s^C under different base surface temperature. If the two

lines in Fig. 5 coincided, L_s would have a linear dependence on surface temperature. However, Fig. 5 shows that only when the base surface temperature is below about $-5°C$ are the differences between $|L_s^{+1} - L_s^C|$ and $|L_s^{-1} - L_s^C|$ so small that the dependence of L_s
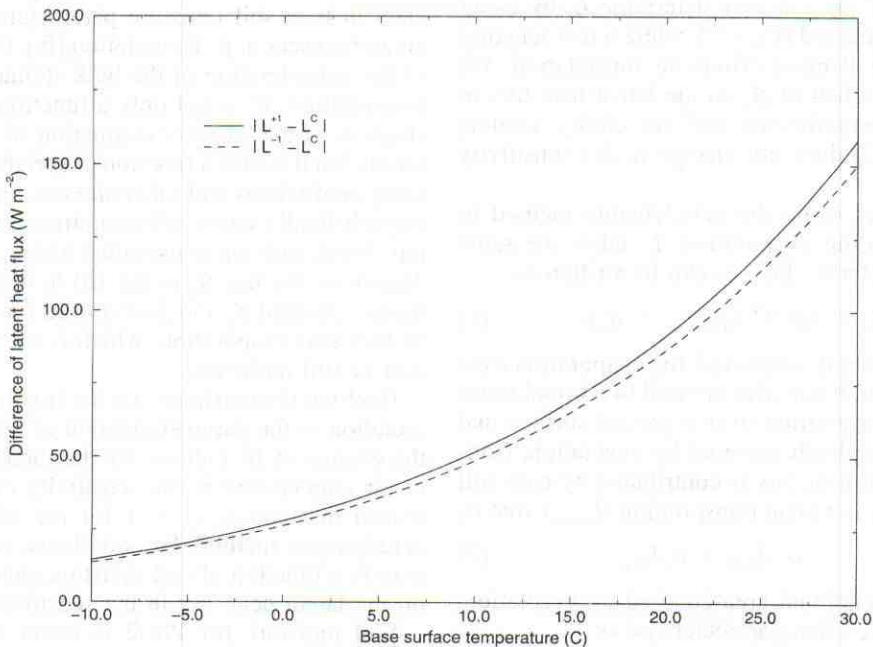

FIG. 5. $|L_s^{+1} - L_s^C|$ and $|L_s^{-1} - L_s^C|$ (W m^{-2}) at different base surface temperatures. Here L_s^{+1} and L_s^{-1} represent the potential evaporation for increasing and decreasing of surface temperature by 1 K from a base surface temperature, respectively. Also, L_s^C is L_s at the base surface temperature.

on T_s is quasi linear. This is not the case for the most of the year in Cabauw: all monthly mean air temperatures in Cabauw are higher than 0°C (Beljaars and Bosveld 1997; Chen et al. 1997).

The interesting point here is that the nonlinear change of L_s with regard to the linear change of temperature is shown in a way that the amount of increase of L_s for $+1$ K T_s is larger than the amount of decrease of L_s for -1 K T_s, that is, $|L_s^{+1} - L_s^{C}| > |L_s^{-1} - L_s^{C}|$. However, in the Cabauw sensitivity experiments $|L^{+2} - L^{C}|$ is much smaller than $|L^{-2} - L^{C}|$ (i.e., $r_L < 1$). This implies that the nonlinear behavior of L in the Cabauw sensitivity experiments cannot be attributed to the nonlinear relationship between T_s and q_* in the formulation of L_s [Eq. (2)] used by the PILPS schemes. As mentioned in section 2a, however, in the Cabauw sensitivity experiments, a so-called β_g formulation is generally involved in the parameterization of L (Shao et al. 1994; Mahfouf and Noilhan 1991; Kondo et al. 1990). The effect of β_g on the relationship between L and T_s has not been considered in the numerical test above. Also not considered in the numerical test above is the effects of the changes in drag coefficient induced by the change of the stratification due to the imposed change of air temperature by ± 2 K. These will be reviewed in the next sections.

3. The formulation of latent heat fluxes in current land-surface parameterizations

a. The β adjustment

As mentioned in section 2a, latent heat flux is commonly parameterized by using Eq. (1) in PILPS schemes. Most of the schemes determine L_s by using the aerodynamic method [Eq. (2)], while a few schemes (Table 1) use the Penman–Monteith formulation. We first consider the effect of β_g on the latent heat flux in these sensitivity experiments and, for clarity, assume drag coefficient C_E does not change in the sensitivity experiments.

For the schemes using the aerodynamic method to determine the scaling evaporation, L_s takes the same form as Eq. (2). Hence, Eq. (1) can be written as

$$L = \beta_g \times \lambda \rho U C_E (q_*(T_s) - q_a). \tag{6}$$

Equation (6) is usually employed for evaporation over bare soil. However, it can also be used in a broad sense for total evapotranspiration over a ground surface that is partially or completely covered by vegetation. Considering that latent heat flux is contributed by bare soil evaporation (L_{soil}) and plant transpiration (L_{plant}), that is,

$$L = (1 - \sigma_f)L_{soil} + \sigma_f L_{plant}, \tag{7}$$

where σ_f is the fractional area covered by vegetation. Here L_{soil}, L_{plant} are often parameterized as

$$L_{soil} = \beta \times \lambda \rho (q_*(T_s) - q_a)/r_a \tag{8}$$

or

$$L_{soil} = \lambda \rho U C_E (\alpha \times q_*(T_s) - q_a) \tag{9}$$

and

$$L_{plant} = \lambda \rho (q_*(T_s) - q_a)/(r_a + r_s), \tag{10}$$

where $r_a = 1/UC_E$ is aerodynamic resistance, r_s is bulk stomatal resistance [note that although T_s and r_a in Eqs. (8), (9), and (10) are different, we simplify and use the same notation here], and β and α are the scaling parameters that are often used for calculating bare soil moisture (Mahfouf and Noilhan 1991; Kondo et al. 1990). Most PILPS schemes use β method, while a few schemes (e.g., ISBA, SSIB) use α method for estimating bare soil evaporation.

After Beljaars and Bosveld (1997), the vegetation cover at Cabauw is close to 100% all year round. Even in winter, after mowing or after a dry spell, it is unusual to see any bare soil. Based on these observations, $\sigma_f > 0.92$ throughout the year was used in the Cabauw experiment (appendix of Chen et al. 1997). Therefore, $(1 - \sigma_f)L_{soil}$ in Eq. (7) can be ignored. Hence,

$$L = \sigma_f L_{plant}$$

$$= \left(\frac{\sigma_f r_a}{r_a + r_s} \right) \times \lambda \rho (q_*(T_s) - q_a)/r_a$$

$$= \beta_g \times \lambda \rho (T_s) - q_a)/r_a, \tag{11}$$

and

$$\beta_g = \frac{\sigma_f r_a}{r_a + r_s}. \tag{12}$$

In this case, we can see that the original scaling parameters in bare soil moisture parameterization, α and β, are not present in β_g formulation [Eq. (12)], and because of the consideration of the bulk stomatal resistance for transpiration, β_g is not only a function of soil moisture stress as is the case for estimation of bare soil evaporation, but it is also a function of aerodynamic resistance (drag coefficient) and other stresses, including the photosynthetically active radiation stress, vapor pressure deficit stress, and air temperature stress, which affect r_s. Therefore, we use β_g in Eq. (6) to distinguish between the generalized β_g and β or α used for parameterization of bare soil evaporation, which is often simply a function of soil moisture.

Here we demonstrate that the involvement of β_g formulation in the parameterization of latent heat flux and the change of β_g induced by the increase and decrease of air temperature in the sensitivity experiments is the reason that causes $r_L < 1$ for the schemes using the aerodynamic method. For simplicity, we assume that β_g is only a function of soil moisture and assess its effects on the latent heat flux in the sensitivity experiments.

Soil moisture for Plus2 is lower than that for the control experiment and that for Minus2, due to the increase of evaporation in Plus2 [see section 3b(3)]. This, therefore, leads to differences in β_g for Plus2 and

TABLE 2. $|L^{+1} - L^c|$ and $|L^{+1} - L^c|$ in the case with and without β_g adjustment.

	+1 K	−1 K	Control	$|L^{+1} - L^c|$		$|L^{-1} - L^c|$
L_s (W m^{-2})	317.5	217.1	265.8	51.7	>	48.7
β_g	0.52	0.75	0.65			
$L_s \times \beta_g$	165.1	162.8	172.8	7.7	<	10.0

Minus2. We include this adjustment in β_g in the numerical test discussed in section 2b by using values from the Cabauw sensitivity experiments. The goal is to see if the inconsistency mentioned above disappears. We assume

$$\beta_g = \min\left(\frac{W_g - W_{wilt}}{W_{cr} - W_{wilt}}, 1\right) \quad (13)$$

(cf. Liang et al. 1994; Pan and Mahrt 1987; Robock et al. 1995), where W_g is soil water content, W_{wilt} is wilting point soil water content, and W_{cr} is the critical soil moisture above which evaporation is not affected by the moisture stress in the soil. Since for most schemes W_g is the root zone soil moisture and the depth of the root zone was prescribed as 1 m in Cabauw experiments, we consider W_g as the soil moisture for the top 1 m in the analysis. For the top 1-m soil layer, we assume here that W_{cr} is 75% of Manabe's (1969) effective water capacity (150 mm) plus the unavailable water content at wilting, W_{wilt} (214 mm) (appendix of Chen et al. 1997). Using monthly values of W_g from BASE output, annual mean values of β_g are calculated. These are 0.52, 0.75, and 0.65 for Plus2 (β_g^{+2}), Minus2 (β_g^{-2}), and the control experiment (β_g^C), respectively. These values are used to adjust the L_s from the numerical test discussed in section 2b [Eq. (2)], that is, to calculate $L_s \times \beta_g$:

$$L^{+1} = L_s^{+1} \times \beta_g^{+2},$$
$$L^{-1} = L_s^{-1} \times \beta_g^{-2},$$
$$L^C = L_s^C \times \beta_g^C. \quad (14)$$

Table 2 gives L^{+1}, L^{-1}, and L^C for an arbitrary base temperature, $T_s = 283$ K. It can be seen that, after adjusting L with β_g, the relation is shifted, that is, $|L^{+1} - L^c|$ is smaller than $|L^{-1} - L^c|$. This is then consistent with the situation in Cabauw sensitivity experiments. It is clearly shown that β_g has a profound effect on the performance of L. This becomes still clearer if we replot Fig. 5 with L adjusted by β_g.

Figure 6 shows $|L^{+1} - L^c|$ and $|L^{-1} - L^c|$ at different base surface temperatures and for two different sets of β_g value. In Fig. 6a, the β_g values in Table 2 are used, that is, $\beta_g^{+2} = 0.52$, $\beta_g^{-2} = 0.75$, $\beta_g^C = 0.65$. It can be seen that $|L^{+1} - L^c| < |L^{-1} - L^c|$ when the surface temperature is between about −3° and 10°C. If we artificially tune β_g (i.e., assume $\beta_g^{+2} = 0.46$, $\beta_g^{-2} = 0.70$, $\beta_g^C = 0.54$), but still keep $\beta_g^{+2} < \beta_g^C < \beta_g^{-2}$, that is, accepting that modeled soil moisture for Plus2 is lower
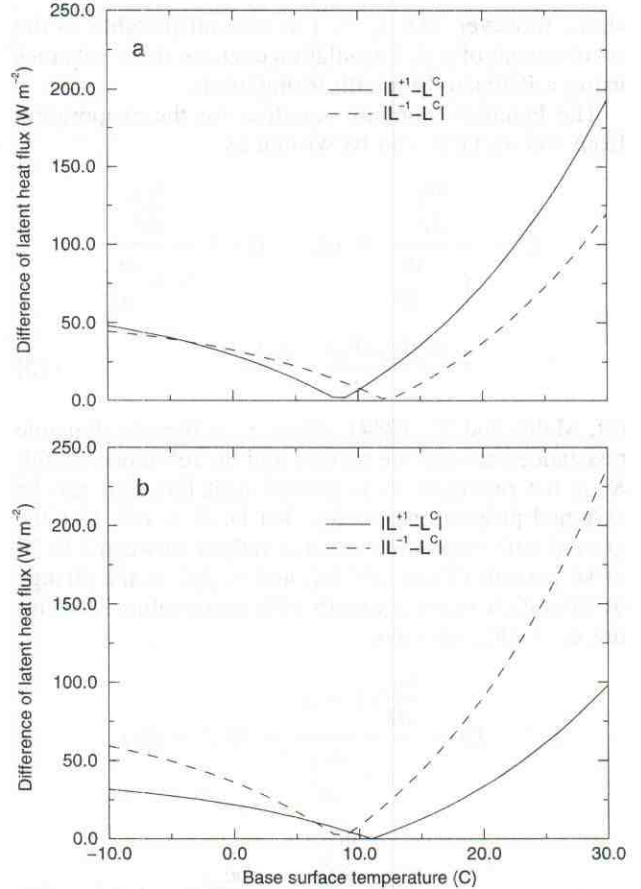

FIG. 6. $|L^{+1} - L^c|$ and $|L^{-1} - L^c|$ (W m^{-2}) at different base surface temperature. The meaning of L^{+1}, L^{-1}, and L^c is same as those in Eq. (14). Different values of β_g are used and in (a): β_g set from Table 2 (i.e., $\beta_g^{+2} = 0.52$, $\beta_g^{-2} = 0.75$, $\beta_g^C = 0.65$); in (b): artificially tuned β_g set ($\beta_g^{+2} = 0.46$, $\beta_g^{-2} = 0.70$, $\beta_g^C = 0.54$).

than that for the control experiment and that for Minus2 is higher than the control experiment, it can be seen that $|L^{+1} - L^c|$ is generally less than $|L^{-1} - L^c|$, except for a small range around a surface temperature of about 7°C but which itself depends on the value of β_g (Fig. 6b). The location of this temperature range, here 7°C, is arbitrary, depending on q_a chosen for the test. It happens here that q_* at the points around 7°C is nearly equal to q_a.

The analysis above shows that the involvement of the β_g formulation in the parameterization of latent heat flux causes the nonlinearity of L with regard to the linear change of air temperature in the form that the increase of latent heat flux in Plus2 is much smaller than its decrease in Minus2, that is, $r_L \ll 1$. Without the involvement of the β_g formulation, the nonlinearity is different, namely, the increase of latent heat flux in Plus2 is larger than its decrease in Minus2, as discussed in section 2b.

For the schemes using the Penman–Monteith formulation to determine the scaling evaporation, the situation is more complicated. The following analysis will

show, however, that $r_L < 1$ is still attributable to the involvement of a β_g formulation even for those schemes using a Penman–Monteith formulation.

The Penman–Monteith equation for the evaporation from wet surfaces can be written as

$$L_s = \frac{\dfrac{\partial e_*}{\partial T}}{\gamma + \dfrac{\partial e_*}{\partial T}} \times (R_n - G) + \frac{\dfrac{\partial e_*}{\partial T}}{\gamma + \dfrac{\partial e_*}{\partial T}}$$

$$\times \frac{\rho c_p (e_*(T_a) - e_a)}{r_a} \qquad (15)$$

(cf. Mahrt and Ek 1984), where r_a is the aerodynamic resistance between the surface and the reference height; R_n is net radiation, G is ground heat flux that can be assumed proportional to R_n, that is, $G = aR_n$ [for the ground with vegetation cover, a ranges between 2 to 20 or so percent (Thom 1975)]; and $\partial e_*/\partial T$ is the change of saturation vapor pressure with temperature. Assuming $G = aR_n$, we have

$$L_s^{+2} - L_s^C = \frac{\dfrac{\partial e_*}{\partial T}(1 - a)}{\gamma + \dfrac{\partial e_*}{\partial T}} \times (R_n^{+2} - R_n^C)$$

$$+ \frac{\dfrac{\partial e_*}{\partial T}}{\gamma + \dfrac{\partial e_*}{\partial T}} \times \frac{\rho c_p}{r_a}[e_*^{+2} - e_*^C] \quad (16)$$

and

$$L_s^{-2} - L_s^C = \frac{\dfrac{\partial e_*}{\partial T}(1 - a)}{\gamma + \dfrac{\partial e_*}{\partial T}} \times (R_n^{-2} - R_n^C)$$

$$+ \frac{\dfrac{\partial e_*}{\partial T}}{\gamma + \dfrac{\partial e_*}{\partial T}} \times \frac{\rho c_p}{r_a}[e_*^{-2} - e_*^C], \quad (17)$$

where $e_*^{+2} = e_*(T_a + 2)$, $e_*^{-2} = e_*(T_a - 2)$ and $e_*^C = e_*(T_a)$. Since the net radiation is given by

$$R_n = (1 - \alpha_s)R_s + R_L\downarrow - R_L\uparrow, \qquad (18)$$

where R_s is shortwave solar radiation, α_s is surface albedo, $R_L\downarrow$ is downward longwave radiation, and $R_L\uparrow$ is upward longwave radiation. In the sensitivity experiments, R_s and $R_L\downarrow$ are the same as those in the control experiment. In Plus2 and Minus2, α_s changes in the winter months due to the change in snow cover induced by 2 K increase or decrease of air temperature. However, this change is quite small (Qu et al. 1996), and on the annual average it can be neglected; that is, we assume

that $(1 - \alpha_s)R_s$ in Plus2 and Minus2 is also same as that in the control experiment. Hence, we have

$$R_n^{+2} - R_n^C = R_L^C\uparrow - R_L^{+2}\uparrow. \qquad (19)$$

Since the emissivity of the surface was set to unity, we have

$$R_L^{+2}\uparrow = \sigma(T_s^{+2})^4 \qquad (20)$$

and

$$R_L^C\uparrow = \sigma(T_s^C)^4, \qquad (21)$$

where σ is the Stefan–Boltzmann constant, and T_s^C and T_s^{+2} are the surface temperatures in the control and sensitivity experiments, respectively. If we write $(T_s^{+2} - T_s^C) = \Delta T_s^+$, Eq. (19) can be expressed as

$$R_n^{+2} - R_n^C = \sigma[T_s^4 - (T_s + \Delta T_s^+)^4]$$

$$= -\sigma[4T_s^3\Delta T_s^+ + 6T_s^2(\Delta T_s^+)^2 + \cdots]$$

$$\approx -4\sigma T_s^3\Delta T_s^+(1 + 6\Delta T_s^+/4T_s), \qquad (22)$$

where negligible terms in $(\Delta T_s^+)^3$ and $(\Delta T_s^+)^4$ are omitted. The value ΔR_n can therefore be expressed as

$$R_n^{+2} - R_n^C = -4\sigma T_s^3\Delta T_s^+, \qquad (23)$$

with an error given by $1.5\Delta T_s^+/T_s$. For $T_s = 298$ K, the error is only 0.5% per degree temperature difference. Using Eq. (23), Eqs. (16) and (17) can be rewritten as

$$L_s^{+2} - L_s^C = \frac{\dfrac{\partial e_*}{\partial T}(1 - a)}{\gamma + \dfrac{\partial e_*}{\partial T}} \times (-4\sigma T_s^3\Delta T_s^+)$$

$$+ \frac{\dfrac{\partial e_*}{\partial T}}{\gamma + \dfrac{\partial e_*}{\partial T}} \times \frac{\rho c_p}{r_a}[e_*^{+2} - e_*^C] \quad (24)$$

and

$$L_s^{-2} - L_s^C = \frac{\dfrac{\partial e_*}{\partial T}(1 - a)}{\gamma + \dfrac{\partial e_*}{\partial T}} \times (-4\sigma T_s^3\Delta T_s^-)$$

$$+ \frac{\dfrac{\partial e_*}{\partial T}}{\gamma + \dfrac{\partial e_*}{\partial T}} \times \frac{\rho c_p}{r_a}[e_*^{-2} - e_*^C], \quad (25)$$

where $\Delta T_s^+ = T_s^{+2} - T_s^C$ and $\Delta T_s^- = T_s^{-2} - T_s^C$. In Eqs. (24) and (25), small changes of γ, ρ, c_p, and $\partial e_*/\partial T$ are neglected. Therefore, without the β_g adjustment, the ratio $r_{Ls} = |(L_s^{+2} - L_s^C)/(L_s^{-2} - L_s^C)|$ is dependent on ΔT_s^+, ΔT_s^-, $e_*^{+2} - e_*^C$, and $e_*^{-2} - e_*^C$. As the signs of the first and second term of the right-hand side in Eqs. (24) and (25) are opposite, r_{Ls} could be smaller than 1. How-

ever, since $|\Delta T_s^+| \approx |\Delta T_s^-|$ (Fig. 1) and $|e_*^{+2} - e_*^C|$ is always larger than $|e_*^{-2} - e_*^C|$ because the function $e_*(T)$ is convex, $r_{L,s}$ is in fact larger than 1. Therefore, for the schemes using the Penman–Monteith formulation, $r_L < 1$ in the sensitivity experiments can still be also explained by the β_g adjustment as discussed above.

b. Influence of the stress factors on the change of β_g in the sensitivity experiments

From the discussions in section 3a, it can be seen that (i) the involvement of the β_g formulation in the parameterization of latent heat flux and (ii) the change of β_g induced by the change of air temperature is responsible for $r_L < 1$ both for the schemes using the aerodynamic method to determine the scaling evaporation, and for the schemes using Penman–Monteith. As β_g is a function of r_a and a series of stress factors, we will discuss in the following section which factors most strongly influence the change of β_g and therefore the change of latent heat flux in the sensitivity experiments.

1) THE INFLUENCE OF AIR TEMPERATURE ON DRAG COEFFICIENT

As drag coefficient C_E (some models use alternatively aerodynamic resistance) for water vapor transfer, which is involved in β_g [Eq. (11)], depends on thermal stability, increasing or decreasing forcing air temperature also influences C_E. The following analysis shows that the changes in C_E induced by air temperature changes of ± 2 K have a significant influence on monthly or annual latent heat flux for most of the schemes.

Figure 7a shows the diurnal variation of the bulk Richardson number [$Ri = gz/T \times (T_a - T_s)/U^2$, $T = (T_a + T_s)/2$], calculated by using T_s from BATS for Plus2, Minus2, and the control experiment for the time from 10 to 13 September (see Chen et al. 1997 for details). It can be seen that the differences of the calculated Richardson number between Plus2 and control and also between Minus2 and control are quite small during the day but larger at night. This is due to the smaller difference between air temperature and surface temperature induced by strong dependence of surface temperature on absorbed solar radiation during the day. Using the calculated bulk Richardson number, the drag coefficient C_E can be estimated after Mahrt and Ek (1984) (Fig. 7b). From this estimation, C_E^C/C_E^{+2} and C_E^{-2}/C_E^C can be calculated, where C_E^C, C_E^{+2}, and C_E^{-2} are C_E for control, Plus2, and Minus2, respectively. The values of C_E^C/C_E^{+2} and C_E^{-2}/C_E^C have a quite large diurnal variation, but for most of the daytime both C_E^C/C_E^{+2} and C_E^{-2}/C_E^C are around 1.5. We therefore assume that $C_E^C/C_E^{+2} \approx 1.5$, that is, $r_a^{+2}/r_a^C \approx 1.5$, and $C_E^{-2}/C_E^C \approx 1.5$, that is, $r_a^C/r_a^{-2} \approx 1.5$ where r_a^C, r_a^{+2}, and r_a^{-2} are r_a for control, Plus2, and Minus2, respectively. The relative change of latent heat flux for Plus2 can then be estimated by using Eq. (11) and the relation $r_a^{+2}/r_a^C \approx 1.5$,

$$\frac{\Delta L^{+2}}{L} = \left| \frac{L^C - L^{+2}}{L^C} \right|$$

$$= \left| 1 - \frac{q_*^{+2} - q_a}{q_*^C - q_a} \times \frac{\sigma_f/(1.5r_a^C + r_s)}{\sigma_f/(r_a^C + r_s)} \right|, \quad (26)$$

where $\Delta L^{+2}/L$ is the relative change of latent heat flux induced by the change of drag coefficient due to the change of stratification when air temperature is increased by 2 K in Plus2. Here q_*^{+2} and q_*^C are q_* at T_s^{+2} and T_s^C, respectively. Note that σ_f in Eq. (26) does not change between Plus2, Minus2, and control. Using a typical value of $(q_*^{+2} - q_a)/(q_*^C - q_a) = 1.3$ for Cabauw in Eq. (26), we have

$$\frac{\Delta L^{+2}}{L} = \left| \frac{L^C - L^{+2}}{L^C} \right| = \left| 1 - 1.3 \times \frac{r_a^C + r_s}{1.5r_a^C + r_s} \right|. \quad (27)$$

Similarly, we have the relative change of latent heat flux for Minus2:

$$\frac{\Delta L^{-2}}{L} = \left| \frac{L^C - L^{-2}}{L^C} \right|$$

$$= \left| 1 - \frac{q_*^{-2} - q_a}{q_*^C - q_a} \times \frac{\sigma_f/(0.67r_a^C + r_s)}{\sigma_f/(r_a^C + r_s)} \right|. \quad (28)$$

Using a typical value of $(q_*^{-2} - q_a)/(q_*^C - q_a) = 0.8$, we have

$$\frac{\Delta L^{-2}}{L} = \left| \frac{L^C - L^{-2}}{L^C} \right| = \left| 1 - 0.8 \times \frac{r_a^C + r_s}{0.67r_a^C + r_s} \right|. \quad (29)$$

We examine how the relative change of L in Plus2 differs from that in Minus2. In fact, $r_L = (\Delta L^{+2}/L)/(\Delta L^{-2}/L)$, that is,

$$r_L = \frac{\left| \dfrac{L^C - L^{+2}}{L^C} \right|}{\left| \dfrac{L^C - L^{-2}}{L^C} \right|} = \frac{\left| 1 - 1.3 \times \dfrac{r_a^C + r_s}{1.5r_a^C + r_s} \right|}{\left| 1 - 0.8 \times \dfrac{r_a^C + r_s}{0.67r_a^C + r_s} \right|}. \quad (30)$$

Figure 8 shows r_L as a function of r_a and r_s after Eq. (30). It can be seen from Fig. 8 that r_L decreases with the increase of r_a and the decrease of r_s. This implies that for the schemes with explicit stomatal control, the involvement of bulk stomatal resistance r_s reduces the influence of the change of r_a on L. However, it can be seen from Eq. (30) that accounting only for the effects of temperature on q_*,

$$r_L = \frac{|1 - 1.3|}{|1 - 0.8|} = 1.5. \quad (31)$$

Since the daily mean r_a in Cabauw is lower than 40 s m^{-1} for most of the year, we assume $r_a = 30$ s m^{-1}. Because the observed midday average of r_s for Cabauw ranges from about 0–120 s m^{-1} through the entire year
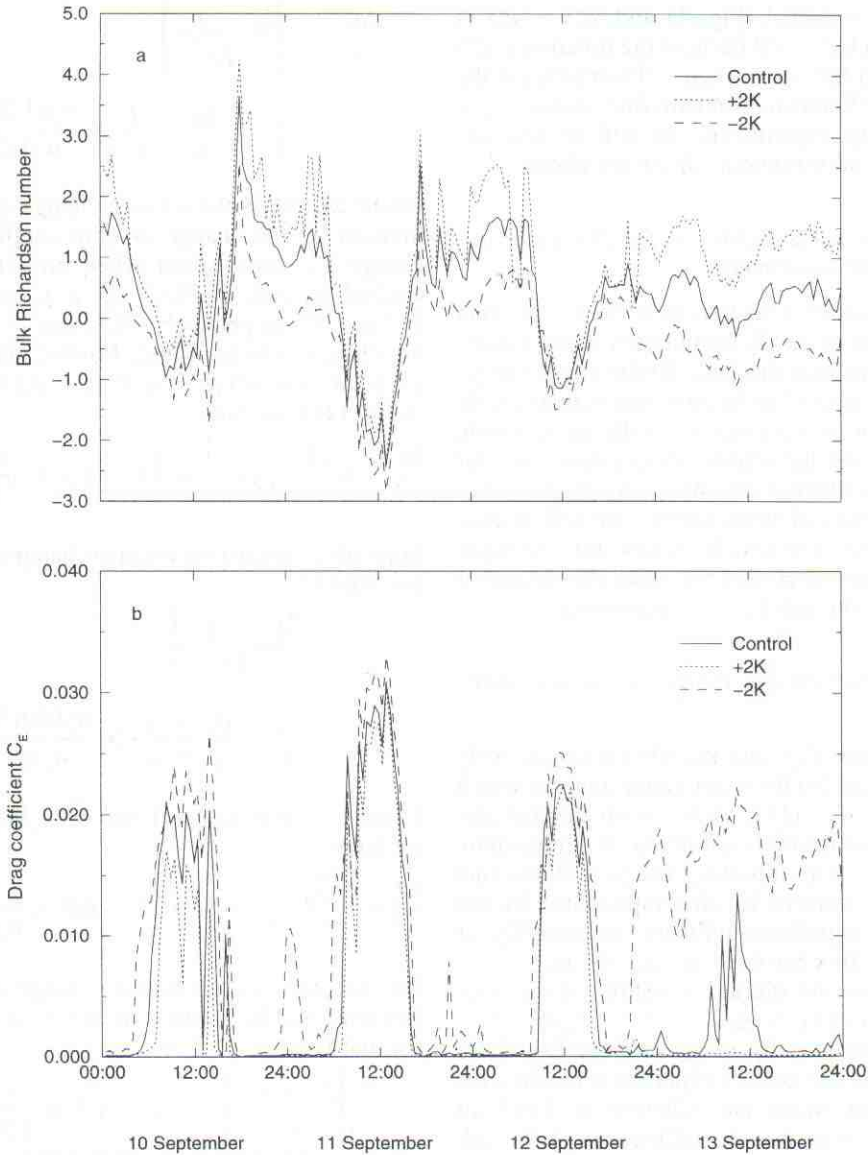
FIG. 7. Diurnal variation of (a) bulk Richardson number and (b) drag coefficient C_E, calculated after Mahrt and Ek (1984) for BATS (10–13 September 1987).
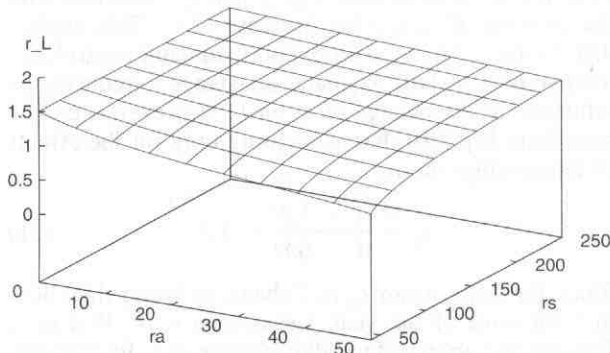

FIG. 8. r_L as a function of r_a (s m^{-1}) and r_s (s m^{-1}) after Eq. (30).

(Beljaars and Bosveld 1997) and the mean value is about 60 s m^{-1}, we assume $r_s = 60$ s m^{-1} here. Using these values in Eq. (30), we then have $r_L = 1.1$. This accounts for the change in q_* and the change in r_a. The model average of $r_L = 0.57$, which can be considered as r_L accounting for change in q_*, r_a, and r_s. We can see from simple estimations above that the changes due to r_s appear to be only slightly larger than those due to r_a. This implies that drag coefficient effects in these sensitivity experiments have the same order of importance as the r_s effects, which will be discussed in the following sections.

It should be noted that for a cloudy day with lower net radiation, the differences of the calculated Richardson number between Plus2 and control and also between
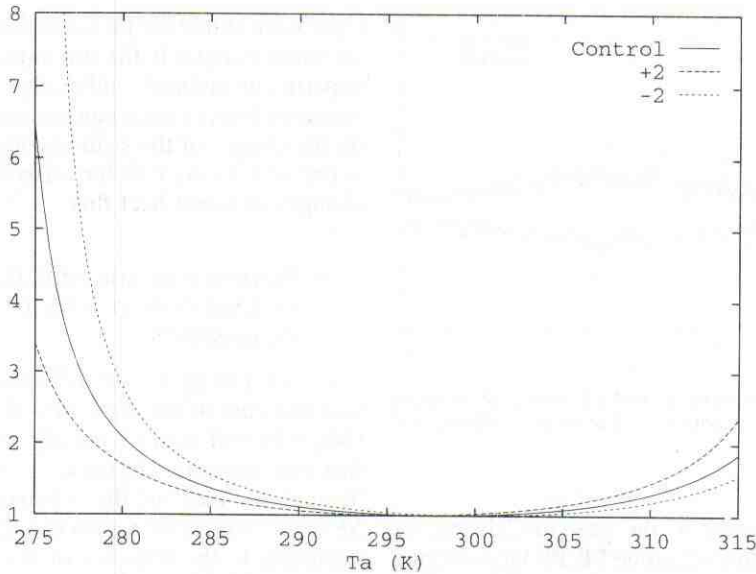
FIG. 9. The variation of the temperature stress factor S_f^{-1} with the temperature for
control, Plus2, and Minus2.

Minus2 and control could be quite large during the day, such as on 13 September. For Plus2, for example, C_E^C/C_E^{+2} could be as large as 3. This may result in a higher relative change of latent heat flux being up to 50%. In this case, however, latent heat flux is also small (the daily mean L on 13 September is about 26 W m^{-2}, which is only about 60% of annual mean L) due to the smaller energy available for evaporation (for 13 September, daily mean R_n < 18 W m^{-2}) and therefore makes only a small contribution to the monthly or annual latent heat flux.

It should be pointed out that for the models without explicit stomatal control of transpiration and with no or small changes in predicted soil moisture for Plus2 and Minus2, the change in C_E may play a dominant role in resulting r_L < 1. Models SPONSOR and SWAP are examples of this situation. The transpiration in these two models is estimated by modifying potential evaporation through a β_T formulation that is a function of soil moisture only. Since the predicted soil moisture for Plus2, Minus2, and control is nearly the same and larger than W_{cr} [see section 3b(3)], β_T is nearly the same for Plus2, Minus2, and control. Therefore, r_L < 1 is mainly caused by decreases in C_E induced by the more unstable stratification in Plus2 in the calculation of the potential evaporation.

2) INFLUENCE OF AIR TEMPERATURE ON BULK STOMATAL RESISTANCE

The surface resistance (bulk stomatal resistance) involved in β_g is usually represented in land-surface schemes as

$$r_s = \frac{r_{s,min}}{LAI} R_f S_f^{-1} V_f^{-1} M_f^{-1} \qquad (32)$$

(e.g., Noilhan and Planton 1989), where R_f, S_f, V_f, and M_f represent the dependence of r_s on solar radiation, air temperature, vapor pressure, and soil moisture, respectively; LAI is canopy leaf area index. The factor R_f measures the influence of the photosynthetically active radiation. As this does not change in Plus2 and Minus2, R_f also should not change.

The factor S_f introduces an air temperature dependence in the surface resistance. The parameterization of S_f is based on the fact that there is an optimal temperature for plant physiological processes that ranges from about 10° to 40°C. If the temperature is in this range, there is no (or small) temperature stress and S_f^{-1} is equal, or close, to 1. If the temperature is outside this range, it is likely to be a stress factor for the physiological processes of vegetation (here transpiration); hence S_f^{-1} will be larger than 1, that is, r_s will increase [Eq. (32)]. An example of S_f parameterization following Dickinson (1984) is given as follows:

$$S_f^{-1} = \frac{1}{[1.0 - 0.016(298.0 - T_a)^2]}. \qquad (33)$$

Figure 9 gives the variation of S_f^{-1} as a function of air temperature for control ($T_a = T_a$), Plus2 ($T_a = T_a + 2$), and Minus2 ($T_a = T_a - 2$) after Eq. (33). For $T_a = 285$ K, for example, S_f for Plus2 decreases only about 10% compared to control, that is, r_s may decrease about 10%. In this case, the change of latent heat flux is less than 10% [cf. Eq. (11)]. It can be seen that the increase or decrease of air temperature by only 2 K has virtually no, or only a very small, effect on S_f^{-1} and therefore a
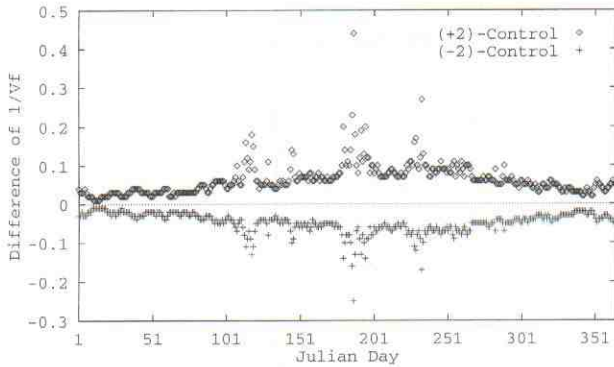
FIG. 10. Calculated daily mean values of the difference of the stress factor V_f^{-1} between Plus2 and control and that between Minus2 and control.

small effect on r_s for most of the year in Cabauw, so that it can be ignored. Indeed, some PILPS land-surface schemes (e.g., SECHIBA, Ducoudre et al. 1993) neglect the influence of air temperature on r_s.

The factor V_f represents the effects of vapor pressure deficit of the atmosphere. Following Jarvis (1976), V_f can be expressed as

$$V_f = 1 - g(e_*(T_a) - e_a), \qquad (34)$$

where g is a species-dependent constant. We take $g = 0.025$ (Noilhan and Planton 1989). It can be seen from Eq. (34) that if air temperature increases vapor pressure deficit will also increase. Hence V_f^{-1} will increase. However, the increase of V_f^{-1} is quite small. Figure 10 shows the calculated daily mean values of the difference of the stress factor V_f^{-1} [Eq. (34)] between Plus2 and control and that between Minus2 and control. It can be seen that the differences of V_f^{-1} between Plus2 and control are within 0.1 for most of the year; that is, r_s may increase by 10% in Plus2 compared to control. In this case, the decrease of latent heat flux is less than 10%. On the other hand, the increase of air temperature will also make $e_*(T_s) - e_a$ increase and this will counteract the stress effect of the increase of vapor pressure deficit. Therefore, the influence of increasing or decreasing air temperature on stress factor V_f can also be neglected for most situations.

Of particular importance is the factor M_f, which accounts for the effects of soil moisture stress on latent heat flux. Usually, M_f varies between 0 and 1 when soil moisture W_g varies between W_{wilt} and W_{cr}. In many schemes, M_f is a simple and explicit function of soil moisture. In some schemes (e.g., ISBA, CSIRO9, and VIC-3L), M_f takes the same form as Eq. (13). The change of predicted soil moisture in Plus2 and Minus2 leads to quite large change in M_f. For example, from the estimation given in section 3a, it can be seen that if M_f takes the form given in Eq. (13), the annual mean of M_f decreases from 0.65 for the control experiment to 0.52 for Plus2. That means an increase of r_s of about 25% for Plus2 compared to control, which will have a

significant influence on latent heat flux. Thus, it can be seen that changes in the soil moisture in these sensitivity experiment induced (indirectly) by the increase or decrease of forcing air temperature plays an important role on the change of the scaling parameter β_g and therefore is one of the major factors affecting the behavior of the changes in latent heat flux.

3) BEHAVIOR OF SOIL MOISTURE AND ITS EFFECT ON LATENT HEAT FLUX IN THE SENSITIVITY EXPERIMENTS

Figure 11a gives the difference of the annual mean soil moisture of the top 1-m soil layer W between Plus2 (Minus2) and control for all schemes. It can be seen that soil moisture decreases in Plus2 and increases in Minus2 for most of the schemes; the exception being SEWAB, which shows no change. This response is attributable to the behavior of latent heat flux, which increases in Plus2 and decreases in Minus2. However, the extent of the decrease (increase) of soil moisture in Plus2 (Minus2) is very different among the PILPS schemes. This can be also seen in Fig. 11b, which gives the absolute value of the difference of soil moisture between Plus2 and Minus2, that is, $|W^{+2} - W^{-2}|$. Some schemes (BASE, BUCKET, CAPS, GISS, ECHAM, PLACE, MOSAIC, CSIRO9, CAPSNMC, VIC-3L) show large $|W^{+2} - W^{-2}|$ over 20 kg m^{-2}, with VIC-3L showing the highest value (85.8 kg m^{-2}). This implies that the soil moisture in these schemes is quite sensitive to the prescribed changes of air temperature. Other schemes (BATS, SSIB, SWAP, SEWAB, SPONSOR) show very small $|W^{+2} - W^{-2}|$, while GISS and MOSAIC show a large increase of soil moisture in Minus2 (37.9 and 29.3 kg m^{-2}, respectively) but only a small decrease in Plus2 (9.6 and 8.9 kg m^{-2}, respectively). Another "outlier" is PLACE, which produces a small increase of soil moisture in Minus2 (9.0 kg m^{-2}) but a large decrease in Plus2 (19.7 kg m^{-2}).

The very small $|W^{+2} - W^{-2}|$ values for BATS, SSIB, SWAP, SEWAB, and SPONSOR are due to the fact that the soil moisture below 1-m depth was prescribed as saturated in these schemes. Since the schemes allow water movement crossing the 1-m interface, the decrease of root zone soil moisture in Plus2 induced by high evaporation under imposed higher air temperature can be compensated by the water supply from the soil below 1 m (water table). For SWAP and SPONSOR, the predicted soil moisture for Plus2, Minus2, and control is in fact nearly the same and near or larger than W_{cr}. There is no straightforward correlation between soil moisture and latent heat flux in terms of their sensitivity to the prescribed changes in air temperature (Figs. 11b,c). For example, both BATS and SSIB show large $|L^{+2} - L^{-2}|$, but very small $|W^{+2} - W^{-2}|$.

As discussed in section 3b(2), for most schemes soil moisture stress factors most strongly influence the change of β_g and therefore the change of latent heat
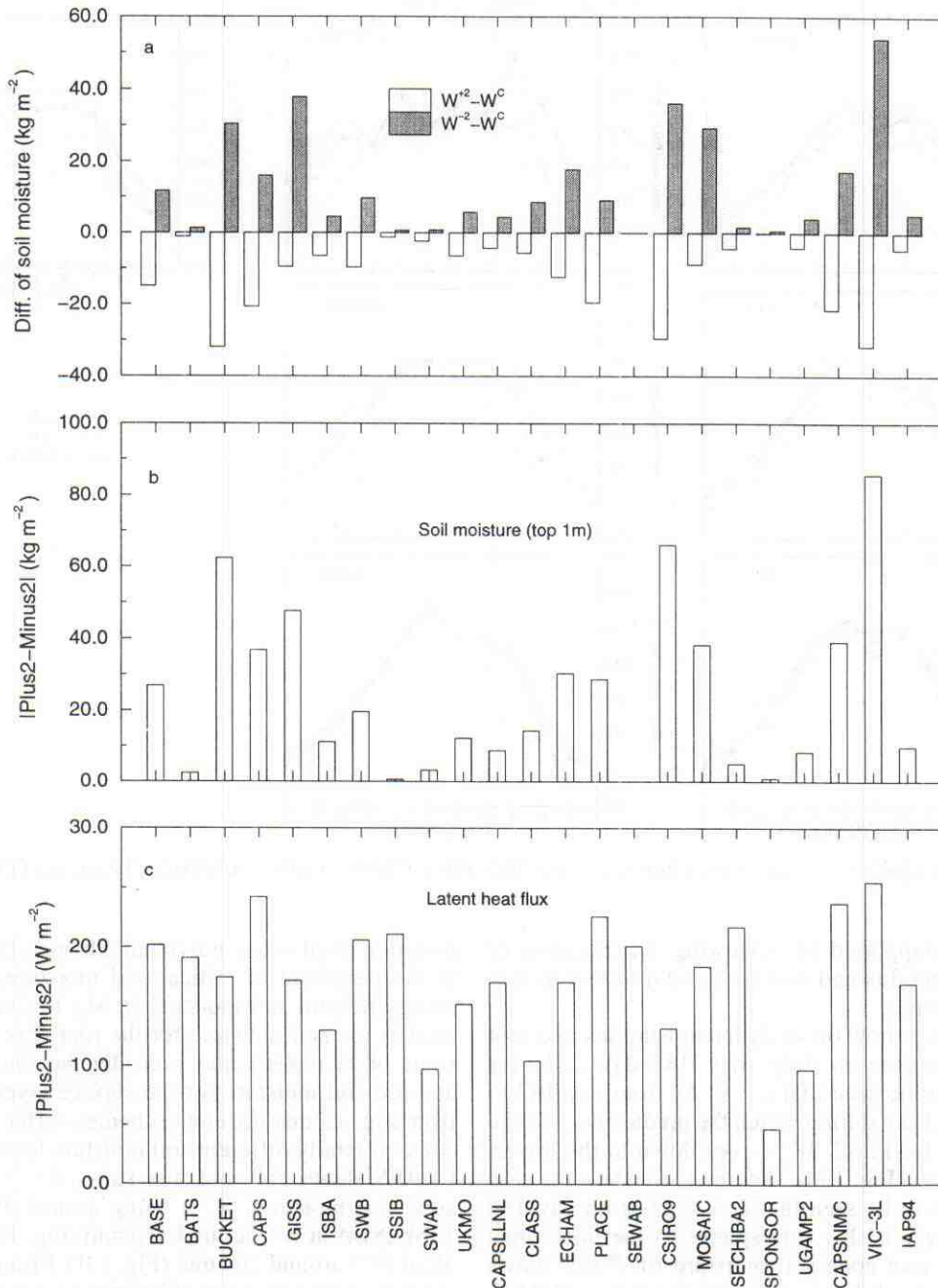
FIG. 11. (a) Difference of soil moisture (kg m^{-2}, top 1 m) between Plus2 and control and that between Minus2 and control, and difference of (b) soil moisture (topmost 1-m soil layer, kg m^{-2}) and (c) latent heat flux (W m^{-2}) between Plus2 and Minus2 for 23 land-surface schemes.

flux in the sensitivity experiments. In Plus2, the decrease of soil moisture under higher temperature ($+2$ K) leads to the decrease of β_g through the decrease of M_f, which is an indication of soil moisture stress, and hence the increase of r_s, which, in turn, leads to lower evaporation.

The effect of the soil moisture stress in Plus2 is quite strong for some schemes, for which monthly latent heat flux for Plus2 is smaller than that for control in summer months. Figure 12 shows the monthly variation of latent

heat flux for BUCKET, CAPS, CAPSNMC, ISBA, CLASS, CSIRO9, and ECHAM. It can be seen in Fig. 12 that monthly mean L of these schemes in Plus2 is lower than or nearly the same as that in the control experiment in summer months, mostly in July. The situation $L^{+2} < L^C$ can only happen when a β_g formulation is involved and L^{+2} is reduced by a small β_g, in which M_f reflects strong soil moisture stress in Plus2 so that L^{+2} is even smaller than or equal to L^C. This argument
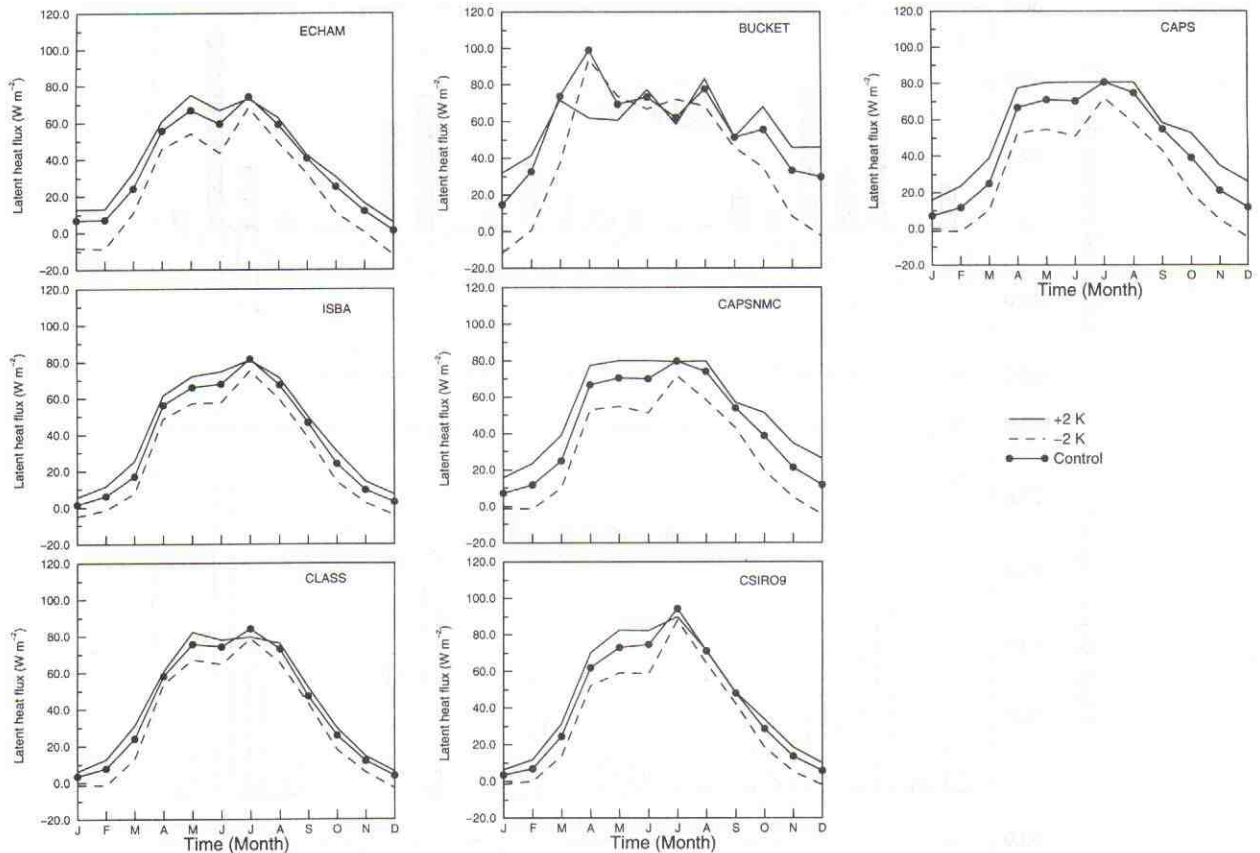
FIG. 12. Monthly variation of latent heat flux of BUCKET, ISBA, CSIRO9, CAPS, CAPSNMC, CLASS, and ECHAM.

seems to be supported by reviewing the variation of daily latent heat flux and root zone soil moisture in July for some schemes.

Figures 13a,b show the daily latent heat flux and root zone soil moisture in July (day 182–day 212) for CLASS. It can be seen that $L^{+2} < L^c$ from day 192 to day 197 (Fig. 13a), during which the predicted root zone soil moisture for Plus2, W^{+2}, goes down to the lowest level of the year (Fig. 13b). Figures 13c,d show the case for ISBA. It can be seen that $L^{+2} < L^c$ from day 186 to day 197, which also corresponds to the time when the predicted root zone soil moisture for Plus2 shows its lowest values of the year. For some schemes (BASE, PLACE, SWB, VIC-3L), although the monthly mean L for July in Plus2 is larger than that in control, the daily latent heat flux for Plus2 is smaller than that for control for some periods in July. Figures 13e,f show the case for VIC-3L as an example. It can be seen that VIC-3L shows $L^{+2} < L^c$ from day 190 to day 197, during which the predicted root zone soil moisture shows its lowest values of the year.

It should be noted that most schemes use different formulations for M_f to describe the limitation of soil moisture to latent heat flux. This implies that different schemes may have different criteria on soil moisture stress, which is caused by (i) differences in M_f for-

mulation involved in individual schemes, (ii) differences in the definition of critical soil moisture, and (iii) by using different soil moisture in M_f; for example, some models use soil moisture for the root zone in M_f, while some other models may consider the root distribution and use soil moisture for the surface layer. We can see from Fig. 13 that different schemes suffer soil moisture stress at totally different soil moisture levels. For Plus2, CLASS shows soil moisture stress ($L^{+2} < L^c$) at root zone soil moisture, W^{+2}, being around 390 mm (Fig. 13b), ISBA at W^{+2} around 310 mm (Fig. 13d), and VIC-3L at W^{+2} around 260 mm (Fig. 13f). From these results we may derive that the difference in the parameterization of the latent heat flux versus soil moisture relationship (both M_f and β for bare soil) across the models might be one of the important reasons for discrepancies among the models. More studies are needed on this issue.

Furthermore, we can also see that the use of the M_f formulation makes it difficult to identify the effect of soil moisture on latent heat flux, because soil moisture has only an indirect relation to latent heat flux through its presence in β_g. In this case, latent heat flux is directly modified by β_g every model time step and is thus sensitive to changes in β_g. Therefore, the formulation of M_f and β (for soil evaporation) parameterizations in β_g
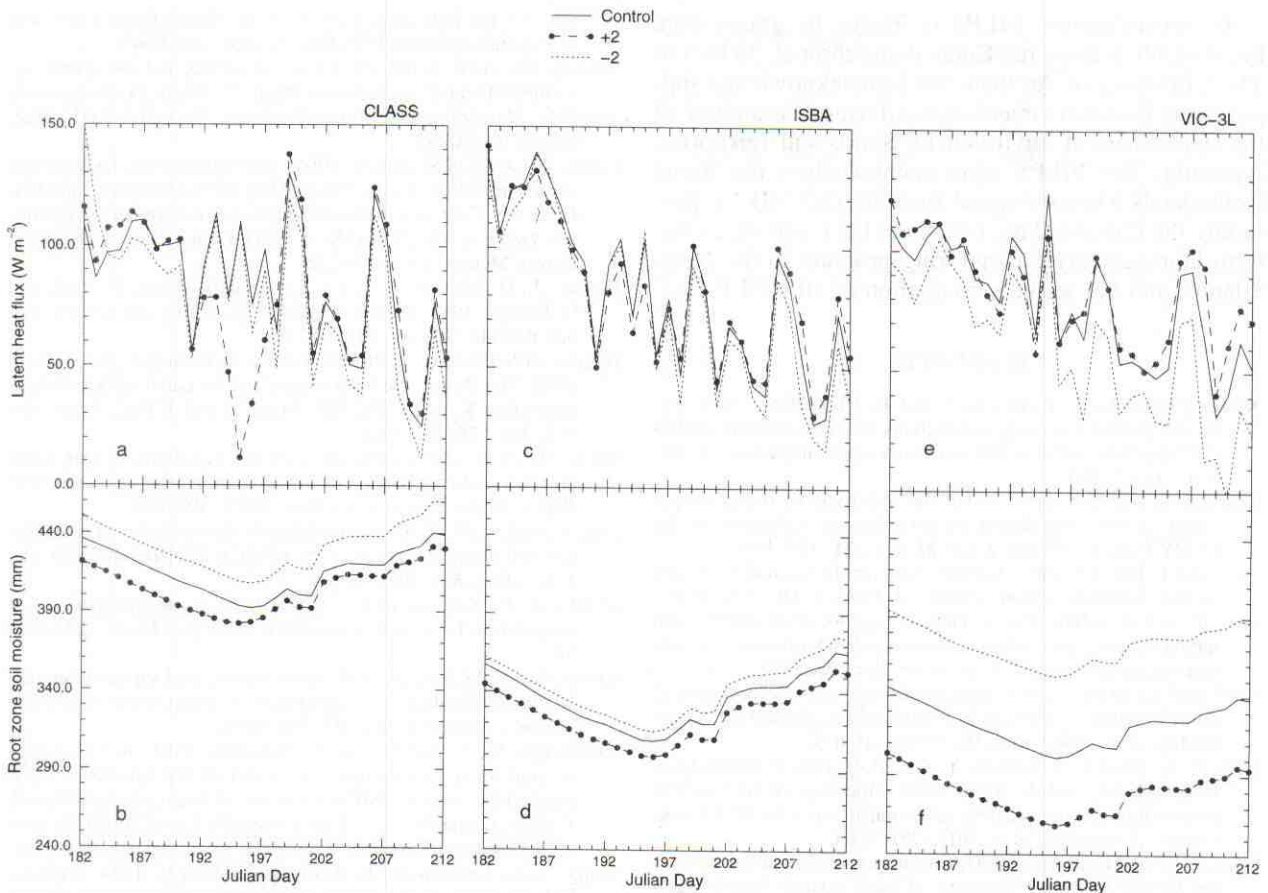
FIG. 13. Daily vacation of latent heat flux for (a) CLASS, (c) ISBA, and (e) VIC-3L for July and daily variation of root zone soil moisture for (b) CLASS, (d) ISBA, and (f) VIC-3L for July.

would have significant influences on predicted latent heat, even if the soil moisture is accurately estimated. This relationship will also become further complicated when the feedbacks between soil moisture and evaporation are considered.

4. Summary and conclusions

Using 23 land-surface schemes, driven off-line by observations from Cabauw, the Netherlands, two sensitivity experiments have been undertaken in which the forcing air temperature was increased or decreased by 2 K and all other parameters remained as in the control experiment. The results show the following.

1) On an annual timescale, all schemes exhibit qualitatively similar and plausible responses to the prescribed 2-K increase or decrease in air temperature, although there are quantitatively significant differences among the schemes. In Plus2 (Minus2), all schemes show that (i) T_s increases (decreases), (ii) latent heat flux increases (decreases), (iii) sensible heat flux decreases (increases), and (iv) soil moisture decreases (increases).
2) The change of latent heat and sensible heat flux is

not linear with respect to the change of air temperature. Specifically, the increase of latent heat flux in the Plus2 experiment is smaller than the decrease of latent heat flux in the Minus2 experiment. This is partly due to the β_g formulation involved in the parameterization of latent heat flux, which is a function of a series of stress factors that limit the scaling evaporation, and partly due to the changes in drag coefficient induced by the change in stratification as a consequence of the imposed change in air temperature (± 2 K).
3) Changes of soil moisture play an important role in the changes of β_g in these sensitivity experiments. For most schemes, one of the reasons for the fact that $|L^{+2} - L^c|$ is much smaller than $|L^{-2} - L^c|$ in the sensitivity experiments is the decrease of soil moisture in Plus2, which leads to a smaller β_g, indicating soil moisture stress. Except for the schemes that specify their soil moisture below 1-m depth as saturated, the effect of soil moisture stress is especially strong for some schemes (BUCKET, CAPS, CAPSNMC, ISBA, CLASS, CSIRO9, ECHAM, BASE, PLACE, SWB, VIC-3L) for which the latent heat flux in Plus2 is even smaller than that in the control experiment in summer months.

REFERENCES

Abramopoulos, F., C. Rosenzweig, and B. Choudhury, 1988: Improved ground hydrology calculations for global climate models (GCMs): Soil water movement and evapotranspiration. *J. Climate,* **1,** 921–941.

Beljaars, A., and P. Viterbo, 1994: The sensitivity of winter evaporation to the formulation of aerodynamic resistance in the ECMWF model. *Bound.-Layer Meteor.,* **71,** 135–149.

——, and F. Bosveld, 1997: Cabauw data for the validation of land surface parameterization schemes. *J. Climate,* **10,** 1172–1193.

Cess, R., and G. Potter, 1988: A methodology for understanding and intercomparing atmospheric climate feedback processes in general circulation models. *J. Geophys. Res.,* **93,** 8305–8314.

——, and Coauthors, 1990: Intercomparison and interpretation of climate feedback processes in 19 atmospheric general circulation models. *J. Geophys. Res.,* **95,** 16 601–16 615.

Chen, F., K. Mitchell, J. Schaake, Y. Xue, H.-L. Pan, V. Koren, Q.-Y. Duan, M. Ek, and A. Betts, 1996: Modeling of land surface evaporation by four schemes and comparison with FIFE observations. *J. Geophys. Res.,* **101,** 7251–7268.

Chen, T.-H., and Coauthors, 1997: Cabauw experimental results from the Project for Intercomparison of Land-surface Parameterization Schemes (PILPS). *J. Climate,* **10,** 1194–1215.

Cogley, J., A. Pitman, and A. Henderson-Sellers, 1990: A land surface for large-scale climate models. Trent University Tech. Note 90-1, 120 pp. [Available from Department of Geography, Trent University, Peterborough, ON K9J 7B8, Canada.]

Dai, Y.-J., and Q.-C. Zeng, 1996: A land surface model (IAP94) for climate studies, Part I: Formulation and validation in off-line experiments. IAP Annual Report, 180 pp. [Available from LASG, Institute of Atmospheric Physics, Chinese Academy of Sciences, Beijing 100080, People's Republic of China.]

Dickinson, R., 1984: Modeling evapotranspiration for three-dimensional global climate models. *Climate Processes and Climate Sensitivity, Geophys. Monogr.,* No. 29, Amer. Geophys. Union, 58–72.

——, A. Henderson-Sellers, P. Kennedy, and M. Wilson, 1986: Biosphere-Atmosphere Transfer Scheme (BATS) for the NCAR community climate model. NCAR Tech. Note NCAR/TN-275+STR, 69 pp. [Available from National Center for Atmospheric Research, Boulder, CO 80303-3000.]

——, ——, and ——, 1993: Biosphere-Atmosphere Transfer Scheme (BATS) version 1e as coupled to the NCAR community climate model. NCAR Tech. Note NCAR/TN-387+STR, 72 pp. [Available from National Center for Atmospheric Research, Boulder, CO 80303-3000.]

Ducoudre, N., K. Laval, and A. Perrier, 1993: SECHIBA, a new set of parameterizations of the hydrologic exchanges at the land–atmosphere interface within the LMD atmospheric general circulation model. *J. Climate,* **6,** 248–273.

Dümenil, L., and E. Todini, 1992: A rainfall-runoff scheme for use in the Hamburg climate model. *Advances in Theoretical Hydrology,* J. P. O'Kane, Ed., Elsevier Science Publishers, 129–157.

Gedney, N., 1995: Development of a land surface scheme and its application to the Sahel. Ph.D. dissertation, University of Reading, 200 pp. [Available from Dept. of Meteorology, University of Reading, Reading RG6 6BB, United Kingdom.]

Gregory, D., and R. Smith, 1994: Canopy surface and soil hydrology. Unified Model Documentation Paper 25, 59 pp. [Available from U.K. Meteorological Office, Bracknell, Berkshire RG12 2SZ, United Kingdom.]

Gusev, Y., and O. Nasonova, 1996: One-dimensional land-surface parameterization scheme for coupling with atmospheric models. *Proc. Int. Conference: Meteorological Processes in the Boundary Layer of the Atmosphere,* Stara Lesna, Slovak Republic, Slovak Meteor. Soc., 110–115.

Hansen, J., D. Johnson, A. Lacis, S. Lebedeff, P. Lee, D. Rind, and G. Russell, 1981: Climate impact of increasing atmospheric carbon dioxide. *Science,* **213,** 957–966.

Henderson-Sellers, A., A. Pitman, P. Love, P. Irannejad, and T. Chen, 1995: The Project for Intercomparison of Land-surface Parameterization Schemes (PILPS): Phases 2 and 3. *Bull. Amer. Meteor. Soc.,* **76,** 489–503.

Jarvis, P., 1976: The interpretation of the variations in leaf water potential and stomatal conductance found in canopies in the field. *Philos. Trans. Roy. Soc. London,* **B273,** 593–610.

Kim, J., and M. Ek, 1995: A simulation of the surface energy budget and soil water content over the HAPEX-MOBILHY forest site. *J. Geophys. Res.,* **100,** 20 845–20 854.

Kondo, J., N. Saigusa, and T. Sato, 1990: A parameterization of evaporation from bare soil surface. *J. Appl. Meteor.,* **29,** 385–389.

Koster, R., and M. Suarez, 1992: Modeling the land surface boundary in climate models as a composite of independent vegetation stands. *J. Geophys. Res.,* **97,** 2697–2715.

Kowalczyk, E., J. Garratt, and P. Krummell, 1991: A soil-canopy scheme for use in a numerical model of the atmosphere—1D stand-alone model. CSIRO Division of Atmospheric Research Technical Paper No. 23, 56 pp. [Available from CSIRO Division of Atmospheric Research, Aspendale, Victoria 3195, Australia.]

Liang, X., D. Lettenmaier, E. Wood, and S. Burges, 1994: A simple hydrologically based model of land surface water and energy fluxes for general circulation models. *J. Geophys. Res.,* **99,** 14 415–14 428.

——, E. Wood, and D. Lettenmaier, 1996: Surface soil moisture parameterization of the VIC-2L model: evaluation and modifications. *Global Planet. Change,* **13,** 195–206.

Mahfouf, J., and J. Noilhan, 1991: Comparative study of various formulations of evaporation from bare soil using in situ data. *J. Appl. Meteor.,* **30,** 1354–1365.

Mahrt, L., and M. Ek, 1984: Comparative study of various formulations of evaporation from bare soil using in situ data. *J. Appl. Meteor.,* **23,** 222–234.

——, and H.-L. Pan, 1984: A two-layer model of soil hydrology. *Bound.-Layer Meteor.,* **29,** 1–20.

Manabe, S., 1969: Climate and the ocean circulation. Part I: The atmospheric circulation and the hydrology of the earth's surface. *Mon. Wea. Rev.,* **97,** 739–774.

Mengelkamp, H.-T., and K. Warrach, 1997: SEWAB—A parameterization of the surface energy and water balance for atmospheric and hydrological models. External Report, GKSS-Forchungszentrum, 42 pp. [Available from GKSS, D-21502 Geesthacht, Germany.]

Noilhan, J., and S. Planton, 1989: A simple parameterization of land surface processes for meteorological models. *Mon. Wea. Rev.,* **117,** 536–549.

Pan, H.-L., and L. Mahrt, 1987: Interaction between soil hydrology and boundary layer development. *Bound.-Layer Meteor.,* **38,** 185–202.

Pitman, A., and Coauthors, 1993: Results from off-line control simulation (Phase1a). GEWEX Tech. Note, IGPO Publication Series No. 7, 47 pp. [Available from Climatic Impacts Centre, Macquarie University, North Ryde, NSW 2109, Australia.]

Qu, W.-Q., A. Henderson-Sellers, A. Pitman, and T.-H. Chen, 1996: Cabauw sensitivity experimental results from the Project for In-

tercomparison of Land-surface Parameterization Schemes. GEWEX Tech. Note, IGPO Publication Series No. 24, 50 pp. [Available from Climatic Impacts Centre, Macquarie University, North Ryde, NSW 2109, Australia.]

Robock, A., K. Vinnikov, C. Schlosser, N. Speranskaya, and Y. Xue, 1995: Use of midlatitude soil moisture and meteorological observations to validate soil moisture simulations with biosphere and bucket models. *J. Climate,* **8,** 15–35.

Schaake, J., V. Koren, Q.-Y. Duan, K. Mitchell, and F. Chen, 1996: Simple water balance model for estimating runoff at different spatial and temporal scales. *J. Geophys. Res.,* **101,** 7461–7475.

Schlesinger, M., and J. Mitchell, 1987: Model projections of the equilibrium climatic response to increased CO_2. *Rev. Geophys.,* **89,** 760–798.

Shao, Y., and A. Henderson-Sellers, 1996: Modeling soil moisture: A project for intercomparison of land-surface parameterization schemes phase 2(b). *J. Geophys. Res.,* **101,** 7227–7250.

——, and Coauthors, 1994: Soil moisture simulation: A report of the RICE and PILPS workshop. GEWEX Tech. Note, IGPO Publication Series No. 14, 179 pp. [Available from Climatic Impacts Centre, Macquarie University, North Ryde, NSW 2109, Australia.]

Shmakin, A., A. Mikhailov, and S. Bulanov, 1993: Parameterization scheme of the land hydrology considering the orography at different spatial scales. *Exchange Processes at the Land Surface for a Range of Space and Time Scales,* H.-J. Bolle, R. A. Feddes, and J. D. Kalma, Eds., IAHS Press, 569–575.

Thom, A. S., 1975: Momentum, mass and heat exchange. *Vegetation and the Atmosphere,* Vol. 1, J. L. Monteith, Ed., Academic Press, 57–109.

Verseghy, D., 1991: CLASS—A Canadian land surface scheme for GCMs, Part I: Soil model. *Int. J. Climatol.,* **11,** 111–133.

——, N. McFarlane, and M. Lazare, 1993: CLASS—A Canadian land surface scheme for GCMs, Part II: Vegetation model and coupled runs. *Int. J. Climatol.,* **13,** 347–370.

Warrilow, D., A. Sangster, and A. Slingo, 1986: Modeling of land surface processes and their influence on European climate. Dynamic Climatology Tech. Note No. 38, 94 pp. [Available from U.K. Meteorological Office, Bracknell, Berkshire RG12 2SZ, United Kingdom.]

Wetherald, R., and S. Manabe, 1988: Cloud feedback processes in a general circulation model. *J. Atmos. Sci.,* **45,** 1397–1415.

Wetzel, P., and A. Boone, 1995: A parameterization for land–atmosphere–cloud exchange (PLACE): Documentation and testing of a detailed process model of the partly cloudy boundary layer over heterogeneous land. *J. Climate,* **8,** 1810–1837.

Xue, Y., P. Sellers, J. Kinter, and J. Shukla, 1991: A simplified biosphere model for climate studies. *J. Climate,* **4,** 345–364.